

受人  
89-6-524  
高研圖書室

UCLA/89/TEP/24  
June 1989

## GAUGE-INVARIANT THREE-GLUON VERTEX IN QCD

John M. Cornwall  
and  
Ioannis Papavassiliou

Department of Physics  
University of California, Los Angeles, CA 90024-1547

**ABSTRACT.** By resumming the Feynman graphs which contribute to any gauge-invariant process we explicitly construct, at one-loop order, a three-gluon vertex for QCD which is completely independent of the choice of gauge. This vertex satisfies a Ward identity of the type encountered in ghost-free gauges, relating the vertex to the proper self-energy of a previously-constructed gluon propagator, also found by resumming graphs; like the vertex, this self-energy is completely gauge-invariant. We also derive the gauge-invariant propagator and vertex via a second related technique which minimizes the dependence on imbedding these objects in a gauge-invariant process; the same results are found as in the first technique. These results motivate a toy model of the nonlinear Schwinger-Dyson equation satisfied by the exact gauge-invariant three-gluon vertex. This model is non-perturbative and has infrared singularities, which we can remove via gluon mass generation; it shows many interesting features expected of QCD, such as a  $\beta$ -function which is not Borel-summable in perturbation theory.

### 1. Introduction.

In lattice-gauge theory one is under no compulsion to fix a gauge, and so no gauge-dependent quantities need be calculated. It seems to be quite the opposite in the continuum, where even gauge-independent objects (e.g., the S-matrix) are conventionally put together from gauge-dependent propagators and vertices. If one could construct these propagators and vertices exactly from their Schwinger-Dyson (SD) equations in some gauge, this would be no problem in principle; the resultant S-matrix would still be exactly gauge-invariant.

Unfortunately, in strongly-coupled gauge theory like QCD, one is forced to make approximations, and this usually results in uncontrollable gauge dependence which infects even ostensibly gauge-invariant quantities.

Some time ago, a program was proposed<sup>1,2</sup> to deal with this dilemma. In essence, the Feynman graphs contributing to a given gauge-invariant process are resummed into new propagators and vertices where the gauge dependence has been reduced to an absolute minimum—that of the free gluon propagator. The proper-self-energy of the new propagator, and the new vertex, are themselves gauge-independent, as are the SD equations which govern these new Green's functions. To be sure, the new SD equations are more complicated than the usual ones because they have extra terms which enforce gauge invariance; nonetheless, it is possible to truncate the SD equations (usually by keeping only a few terms of a dressed-loop expansion) and maintain exact gauge invariance, while at the same time accommodating non-perturbative effects.

One essential aspect of gauge invariance in the SD-equation context is that the new proper self-energy and vertex obey Ward identities: the proper self-energy is conserved, while the divergence of the vertex is expressible in terms of this proper self-energy alone (with no ghost contributions).

The new propagator and vertex constitute a generalization of the running charge  $\bar{g}(k)$ , which is defined by the renormalization group. However, the usual construction of  $\bar{g}$  can only deal with the ultraviolet properties of the gauge theory, and offers no help in understanding the infrared singularities and their cure. That is why the new propagator and vertex are important: They are determined by SD equations which (in principle, at least) are not restricted to the ultraviolet domain, and can tell us how the infrared singularities are removed.

So far the program of finding the new propagator and vertex is incomplete, although useful results have been obtained (e.g., non-perturbative gluon masses for  $T = 0^{1,2}$  and finite- $T^3$  QCD; plasmon decay rate<sup>4</sup> at finite  $T$ ). These earlier works have concentrated on the new propagator, either in perturbation theory or with the gauge technique<sup>5,6,7</sup>, as a substitute for the new vertex. (The gauge technique expresses part of the part of the vertex in terms of the propagator in such a way as to satisfy the Ward identity exactly; the omitted transverse vertex part is unimportant in the infrared, but essential<sup>8,9</sup> to cure overlapping ultraviolet divergences.) Past the gauge technique, which is incomplete, nothing has been said about the new vertex, even in perturbation theory, much less about the SD equation it satisfies.

In this paper we construct the new gauge-invariant three-gluon vertex at one-loop order in perturbation theory. This is no trivial task, because the algebra is complicated and there are more graphs than for the conventional vertex.<sup>10</sup> We also show that this vertex satisfies the desired Ward identity in terms of the new gauge-invariant proper self-energy. The resummation algorithm we use for the construction is not the one originally proposed in Refs. 1, 2, although that would work perfectly well and would give the same results; instead, we resum graphs contributing to the S-matrix<sup>11</sup> for the on-

shell scattering of three test quarks of different masses. The resummation process identifies longitudinal momenta in numerators which act as divergences on vertices. By a Ward identity the vertex divergence is expressed as a difference of inverse propagators, which "pinch" lines in the graph which carry these propagators (see Fig. 1). This S-matrix pinch technique, as we call it, is slightly easier to follow than that of Refs. 1, 2, because certain contributions vanish by virtue of the on-shell condition for the test quarks.

We use the S-matrix pinch technique to show directly that the Ward identity is satisfied, and a yet-more streamlined algorithm to construct the vertex itself. This second algorithm we call the intrinsic-pinch technique, because it deals with the off-shell vertex graphs themselves, with essentially no reference to any gauge-invariant process in which these vertices might be imbedded. The intrinsic-pinch technique is just another (but quicker) way of saying exactly the same thing as does the S-matrix pinch technique, in which certain cancellations between graphs which occur in the latter technique are anticipated; therefore, the terms to be cancelled need not even be written down.

These algorithms are efficiently stated in terms of a decomposition of the bare vertex first given by 't Hooft<sup>12</sup> and later used<sup>13</sup> in eikonal summations of graphs in QCD. This decomposition singles out one part of the three-gluon vertex, which we call  $\Gamma^F$ , to satisfy a simple Ward identity on one line; the other part, called  $\Gamma^P$ , both generates pinches and cancels ghost numerators. The new gauge-invariant vertex and propagator have quite simple expressions in terms of the  $\Gamma^F$  vertices, which makes the Ward identity relating them very simple to see. We emphasize again that this Ward identity makes no reference to ghosts; the only ingredients for constructing any Green's function are gluon propagators and vertices.

The point of doing such one-loop calculations is to look for guidance in devising truncated but still non-perturbative SD equations, making use of the dressed-loop expansions, which are gauge-invariant. As mentioned earlier, some progress has been made for the new propagator with the help of the gauge technique, but we are not aware of any analogous investigations for the new vertex. In this paper we discuss a toy model of the SD vertex equation which is drastically simplified, but retains some features of real QCD: asymptotic freedom, scale invariance at large momentum, and a cubic nonlinearity, corresponding to a one-dressed-loop graph. We concentrate on only one of the several scalar functions which appear in one form of the three-gluon vertex, and retain only terms which couple this function to itself; thus most of the complications due to spin are bypassed. The vertex function of interest is not the proper vertex, but rather this quantity multiplied, on each leg, by the square root of  $\hat{q}^2$ , where  $\hat{d}(q)$  is the gauge-invariant propagator as defined in Section 2. This vertex vanishes at large momentum because of asymptotic freedom, and we can write down a homogeneous SD equation for it, since no counterterms are necessary.<sup>14</sup>

In spite of the absence of counterterms and integrals which need regularization, our toy SD equation has all of the properties that one would expect from perturbative QCD (as well as new non-perturbative phenomena). For massless gluons, the vertex obeys a renormalization-group equation with  $\beta$ -function of the usual form

$$\beta(g) = -bg^3 - \sum_1^\infty b_N g^{2N+3}. \quad (1.1)$$

Here  $b$  is precisely<sup>15</sup> the usual one-loop coefficient ( $b = 11N (48\pi^2)^{-1}$ ).

Normally one would associate the  $b_N$  with graphs having two or more loops, and

so it is somewhat of a surprise that they appear in our one-dressed-loop model. But the  $b_N$  are there, and they accurately reflect the qualitative properties expected of them in perturbation theory: All are positive, and they show factorial growth at large  $N$ . The coefficient  $b_1$  of  $g^5$  is 80% larger than the exact value, reminiscent of what happens for the coefficient of  $g^3$  in the gauge technique.<sup>15</sup> The positivity of the  $b_N$  prevents Boros-summation of the factorial growth, as long as there is no infrared cutoff for QCD, that is, as long as the gluons are massless.

As far as strict QCD perturbation theory goes, these issues are somewhat delicate, since one can always<sup>16</sup> find a renormalization scheme such that  $b_N = 0$ ,  $n \geq 2$ . In our toy model no ultraviolet-infinite integrals are encountered, and it is very natural to use the specific  $\beta$ -function that we give in Section 4. We can, in fact, characterize  $\beta(g)$  for all  $g$  not by the divergent power series (1.1), but by a first-order nonlinear differential equation for  $\beta$ . Study of this equation shows that  $\beta(g)$  actually has a singular fixed point at  $g \approx 5.3$  ( $\alpha_s \approx 2.2$ ), where  $\beta$  approaches zero with infinite slope. This singularity is associated with infrared divergences of massless QCD, which lead to singularities in the vertex function itself.

It has been argued<sup>1,2</sup> that QCD heals these infrared singularities by a self-consistent process of gluon mass generation, in which the gluon mass  $m$  is induced by soliton condensates in the vacuum; in turn, these solitons exist as nonlinear solutions to the field equations with a (gauge-invariant) mass term added. Evidence for a constituent gluon mass has also been found by lattice-gauge workers,<sup>17</sup> of about the value predicted in Refs. 1, 2. We study this in our toy model for the vertex by changing the massless gluon propagators to massive ones. Singularities persist until the gluon mass  $m$  passes a critical value; roughly  $m/\Lambda_{RG}$  must be of order unity or greater ( $\Lambda_{RG}$  is a typical

renormalization-group mass) for the singularities to disappear. This threshold mass is consistent with earlier studies<sup>1,2</sup> of the gluon propagator equation with the gauge technique. For  $m/\Lambda_{\text{RG}} \approx 2.5$  we find  $\alpha_s(0) \approx 0.5$ , a value typical of fits to quarkonium spectra. For the same value of  $m/\Lambda_{\text{RG}}$ , the running charge as found from the toy model of the vertex equation is about the same as found from the gauge technique for the propagator,<sup>1,2</sup> so there is rough consistency between these two approximations.

We do not expect to find direct evidence for confinement at this level of approximation, even though we are certainly dealing with non-perturbative effects when we add a gluon mass. However, confinement is connected to mass generation, via the vertices which exist<sup>18</sup> for massive gluons. These vertices have long-range pure-gauge parts which confine quarks, but are invisible to gluons, which are screened rather than confined.

For the reader who wishes a quick tour through the paper, the key equations are the Ward identity (2.20) relating the new vertex and the new propagator; (3.9) giving the new propagator; and (3.18) giving the new vertex. The toy model for the vertex SD equation is in Section 4.

## 2. The S-Matrix Pinch Technique.

Here we review this technique as it applies<sup>1,2</sup> to the effective propagator, and then--a very much more complicated exercise--apply it to the gauge-invariant vertex. In each case, the idea is to begin with something known to be gauge-invariant (the S-matrix) and extract from this the corresponding gauge-invariant Green's function. Note that it is the **proper self-energy** and the **proper vertex** which will be gauge-invariant; the propagator has a trivial gauge dependence through the free propagator and this induces an equally trivial dependence in the improper vertex, which is not directly related to the S-matrix.

### A. The Propagator.

Consider the S-matrix element  $T$  for the elastic scattering of two test quarks of masses  $M_1$  and  $M_2$  (see Fig. 1). Evidently, to any order in the coupling  $g$ ,  $T$  is independent of the gauge parameter  $\lambda$ , defined by the free propagator:

$$\Delta_{\mu\nu}(q) = \frac{-q_{\mu\nu} + (1-\lambda) \frac{q_\mu q_\nu}{q^2}}{q^2 + i\epsilon}. \quad (2.1)$$

But the usual propagator graphs (Fig. 1a) are gauge-dependent because the proper self-energy depends on  $\lambda$ . At one-loop level, this dependence is cancelled by other graphs (e.g., Figs. 1b,c), which do not seem to be of propagator type at first glance. In fact, such graphs (and others, if  $\lambda \neq 1$ ) do have propagator-like parts, which we call pinch parts. That this must be so is evident from the form of  $T$ :

$$T(s, t, M_1, M_2) = A(t) + B(t, M_1, M_2) + T_R(s, t, M_1, M_2) \quad (2.2)$$

where (except for trivial external wave functions) the function A depends only on the Mandelstam variable  $t = (p_1 - p_1')^2$ , and not on  $s = (p_1 + p_2)^2$  or on the external masses.<sup>19</sup> The function A(t) is unique<sup>20</sup> and gauge-invariant, and represents the contribution of the new propagator.

We can construct the new propagator  $\hat{A}_{\mu\nu}(q)$  directly from the Feynman rules. In doing so it is evident that we can use any value for  $\lambda$  in (2.1), since A, B, and  $\Gamma_R$  are all independent of  $\lambda$ . The choice  $\lambda = 1$  (Feynman gauge) simplifies the calculation enormously, since only the graph of Fig. 1b (and its mirror image) contribute in this gauge. The pinch part (or propagator part) of this graph arises as follows: up to a group-theoretic factor, the three-gluon vertex in Fig. 1b has the expression

$$\Gamma_{\mu\nu\alpha}^F(-k, -q+k, q) = \Gamma_{\mu\nu\alpha}^F + \Gamma_{\mu\nu\alpha}^P ; \quad (2.3)$$

$$\Gamma_{\mu\nu\alpha}^F = (2k-q)_\alpha q_{\mu\nu} + 2q_\mu q_{\nu\alpha} - 2q_\nu q_{\mu\alpha} ; \quad (2.4)$$

$$\Gamma_{\mu\nu\alpha}^P = -k_\mu q_{\nu\alpha} + (q-k)_\nu q_{\mu\alpha} . \quad (2.5)$$

This decomposition gives a special role to the q-leg in the three-gluon vertex, and provides for  $\Gamma_{\mu\nu\alpha}^F$  to satisfy a Feynman-gauge Ward identity:

$$q^\alpha \Gamma_{\mu\nu\alpha}^F = [k^2 - (q-k)^2] q_{\mu\nu} \quad (2.6)$$

$\Gamma_{\mu\nu\alpha}^F$  is a convective vertex; the other two terms come from gluon spin or magnetic moment. As for  $\Gamma_{\mu\nu}^P$  (P for pinch), it has the property that  $k_\mu$  or  $(q-k)_\nu$  pinches out the internal quark line in Fig. 1b in a Ward identity such

as:

$$k_\mu q_\nu = s^{-1}(p_1 + k) - s^{-1}(p_1) + s^{-1}(p_1 + k) \quad (2.7)$$

where the last form follows because  $p_1$  is on-shell. Thus the contribution of  $\Gamma_{\mu\nu}^P$  is of the form shown in Fig. 1e (and similarly in  $\lambda \neq 1$  gauges, Fig. 1c has a pinch part as shown in Fig. 1f). One can check that  $\Gamma^F$  does not lead to pinch parts.

It is elementary to add the pinch parts to the usual graphs, but one ambiguity needs resolution. Because we are working with the on-shell S-matrix, any terms  $-q_\mu q_\nu$  in the pinch parts do not show up in this quantity (i.e., in A(t)). We define uniquely the proper self-energy associated with the pinch parts by demanding that it be conserved. This means that if the pinch-part proper self-energy has the form

$$\Pi_{\mu\nu}^P(q) = q_{\mu\nu} \Pi^P(q) + -q_\mu q_\nu , \quad (2.8)$$

we define  $\Pi_{\mu\nu}^P$  as

$$\Pi_{\mu\nu}^P = (q_{\mu\nu} - q_\mu q_\nu q^{-2}) \Pi^P(q) . \quad (2.9)$$

This conserved form is, in fact, automatic in other forms of the pinch technique, e.g., the off-shell approach of Refs. 1, 2 or the intrinsic pinch discussed below. At one-loop order, we find

$$\Pi^P(q) = \left[ \frac{1}{2} N \right] \times 2 \times 2 \times \left( \frac{-iq^2}{(2\pi)^4} \right) \int \frac{d^4 k q^2}{k^2 (q+k)^2} =$$

$$= - \frac{2Nq^2}{16\pi^2} q^2 \ln(-q^2/\mu^2) \quad (2.10)$$

where in the second equality we give the renormalized version of the integral.

The factors in front of the integral are a group-theoretic factor  $\frac{1}{2} N = \frac{N}{2}$  (number of colors in  $SU(N)$ ) ; one factor of two for the two terms in  $\Gamma^P$  of (2.5) ; another factor of two because the graph of Fig. 1e has a counterpart with the bubble attached to the lower line. We add  $\hat{\Pi}^P$  to the usual Feynman-gauge proper self-energy

$$\Pi^{(\lambda=1)}(q) = - \frac{5}{3} N \frac{q^2}{16\pi^2} q^2 \ln(-q^2/\mu^2) \quad (2.11)$$

to find the gauge-invariant combination  $-b q^2 \ln(-q^2/\mu^2)$ , where

$$b = \frac{11N}{48\pi^2} \quad (2.12)$$

is the coefficient of  $-q^3$  in  $\beta(q)$ .

We define the new propagator  $\hat{\Delta}_{\mu\nu}(q)$  by

$$\hat{\Delta}_{\mu\nu}^{-1}(q) = \hat{\Delta}_{\mu\nu}^{(o)-1}(q) - \hat{\Pi}_{\mu\nu}(q) \quad (2.13)$$

$$\hat{\Delta}_{\mu\nu}^{(o)-1}(q) = -q^2 g_{\mu\nu} + q_\mu q_\nu (1-\lambda^{-1}) \quad (2.14)$$

$$\begin{aligned} \hat{\Pi}_{\mu\nu}(q) &= \Pi_{\mu\nu}^o(q) + \Pi_{\mu\nu}^P(q) \\ &= (g_{\mu\nu} - q_\mu q_\nu^{-2}) \hat{\Pi}(q) \end{aligned} \quad (2.15)$$

Here  $\Pi_{\mu\nu}^o$  is the sum of the ordinary proper self-energy graphs, and  $\Pi_{\mu\nu}^P$  is the

pinch part. Each of these self-energies is separately conserved, which has the well-known consequence that  $\hat{\Delta}_{\mu\nu}$  has only a trivial gauge dependence:

$$\hat{\Delta}_{\mu\nu}(q) = \frac{-q_\mu q_\nu \hat{\Pi}^2}{q^2 - \hat{\Pi}(q)} - \frac{\lambda q_\mu q_\nu}{q^4} \quad (2.16)$$

since  $\hat{\Pi}$  is independent of  $\lambda$ . For notational convenience we define

$$P_{\mu\nu}(q) = -q_{\mu\nu} + q_\mu q_\nu^{-2} ; \quad (2.17)$$

$$\hat{d}(q) = (q^2 - \hat{\Pi}(q))^{-1} \quad (2.18)$$

so that

$$\hat{\Delta}_{\mu\nu} = P_{\mu\nu} \hat{d} - \frac{\lambda q_\mu q_\nu}{q^4} , \quad (2.19)$$

with  $\hat{d}^{-1} = q^2 (1 + b q^2 \ln(-q^2/\mu^2))$  at one-loop order.

### B. The Gauge-Invariant Vertex.

This calculation is much more tedious than that for the propagator, and for the most part we will only give the reader a roadmap of the way the vertex is constructed and the proof that it satisfies the needed Ward identity.

Our calculations, although they begin with an improper vertex (with  $\hat{\Delta}_{\mu\nu}^o(q_1, q_2, q_3)$ , which at tree level is the usual vertex (2.3) from which we omit a group-theory factor  $i\varepsilon_{abc}$ ), we will construct  $\hat{\Gamma}$  at the one-loop level and show that it obeys

$$q_1 \hat{\Gamma}_{\mu\nu\alpha}(q_1, q_2, q_3) =$$

$$= P_{V\alpha}(q_2) \hat{\Gamma}^{-1}(q_2) - P_{V\alpha}(q_3) \hat{d}^{-1}(q_3) \quad (2.20)$$

with similar Ward identities upon multiplication of  $\hat{\Gamma}_{\mu\nu}$  by  $q_2^\nu$  or  $q_2^\alpha$ . Note that (except in ghost-free gauges<sup>1,2</sup>) the RHS of (2.20) is not the difference of two inverse propagators, because the projection operators  $P_\mu^\nu$  have no inverses. Note also that (2.20) makes no reference to ghost Green's functions, as the usual covariant-gauge Ward identities do; (2.20) is completely gauge-invariant.

As with the propagator  $\hat{\Delta}_{\mu\nu}$ , by far the simplest case is the Feynman gauge  $\lambda = 1$ , since the fewest number of graphs contribute. This is no loss of generality, since we always work with an S-matrix which is known to be  $\lambda$ -independent.

The S-matrix element in question is the connected S-matrix for scattering of three test "quarks" of arbitrary mass, and the graphs which are relevant in Feynman gauge are shown in Fig. 2. In this figure the quark momenta  $p_i$  and  $p_i \cdot q_i$  are on shell. We can extract an improper vertex by identifying the parts of these graphs which are independent of the quark masses  $M_i$ , that is, by finding the pinch parts identified in Fig. 3. Fig. 2c contributes to the pinch part Fig. 3a, and Figs. 2g,h yield the pinch part of Fig. 3b.

The sum  $T$  of ordinary (including improper) vertex graphs and pinch parts is of the form shown in Fig. 4, and is gauge-invariant. From it we define the proper vertex via<sup>21</sup>

$$\hat{\Gamma} = \bar{u}_1 \gamma_\mu u_2 \bar{u}_2 \gamma_\nu u_3 \bar{u}_3 \gamma_\alpha \hat{\Delta}^{\mu\nu} \quad (1) \quad \hat{\Delta}^{\nu\nu} \quad (2) \quad \hat{\Delta}^{\alpha\alpha} \quad (3) \quad \hat{\Gamma}_{\mu\nu\alpha} \quad (2.21)$$

where the propagator  $\hat{\Delta}$  are the new ones as given in (2.19). Now  $\hat{\Gamma}$  is gauge-invariant, and the trivial gauge dependence of the  $\hat{\Delta}_{\mu\nu}$  in (2.19) does not

appear in  $\hat{\Gamma}$  of (2.21) because the test-quark legs are on the mass shell. It follows that we can recover  $\hat{\Gamma}$  from  $\hat{\Gamma}$  by stripping off the  $\hat{\Delta}_{\mu\nu}$  as if they had no  $q_1 q_\nu$  terms at all, and that  $\hat{\Gamma}$  so defined is gauge-invariant. Just as for the propagator  $\hat{\Delta}$ , there remain ambiguities about possible longitudinal terms (e.g.,  $\sim q_1^\mu$ ) in  $\hat{\Gamma}$  which will not contribute to  $\hat{\Gamma}$ ; we resolve these ambiguities by insisting on full Bose symmetry of  $\hat{\Gamma}$  as well as the satisfaction of the Ward identities (2.20). As also happens with  $\hat{\Delta}$ , other off-shell techniques (Refs. 1, 2 and Section III of the present paper) automatically resolve any longitudinal ambiguities.

Before diving into the complexities of the full calculation of  $\hat{\Gamma}$  we give a quick and simple version which illustrates many of the main issues. In this version we save only ultraviolet divergent terms, i.e., those which after renormalization depend on the renormalization mass  $\mu$ , and assume that the index structure of various terms comes out right. By saving only ultraviolet divergent terms we need not consider the graphs of Figs. 2g,h which are finite (except for infrared divergences when certain momenta vanish). Spin structure aside, the Born graph of Fig. 2a is normalized to 1, and adding the conventional proper vertex graphs Figs. 2d,e,f yields, in the Feynman gauge,

$$\hat{\Gamma} = 1 + \frac{2Nq^2}{48\pi^2} \ln(-q^2/\mu^2) . \quad (2.22)$$

To this must be added three times the usual propagator logarithms of Fig. 2b, namely  $-(15/48\pi^2) Nq^2 \ln(-q^2/\mu^2)$ , and three times the pinch part of Fig. 2c (shown in Fig. 3a), which is  $-(9/48\pi^2) Nq^2 \ln(-q^2/\mu^2)$ . The overall sum is identified with  $\hat{\Gamma}^3$  (modulo inessential powers of  $q^2$ ):

$$(q_1^2 q_2^2 q_3^2) \hat{\Gamma}^3 = 1 - 2bg^2 \ln(-q^2/\mu^2) \quad (2.23)$$

with  $b$  from (2.12) the usual  $\beta$ -function coefficient. Since  $q\hat{\Delta} = 1 - bg^2 \ln(q^2/\mu^2)$ , we conclude that  $\hat{\Gamma} = 1 + bg^2 \ln(-q^2/\mu^2) = (q^2\hat{\Delta})^{-1}$ . This is, of course, gauge-invariant as well as consistent with the Ward identity (2.20), which says that the vertex behaves like an inverse propagator.

There is no reason first to calculate  $\hat{\Gamma}\hat{\Delta}^3$  and then to divide by  $\hat{\Delta}^3$  to get  $\hat{\Gamma}$ . This can be done instead by omitting the normal propagator graphs of Fig. 2b, and subtracting the pinch parts of Fig. 2c (that is, Fig. 3a) rather than adding them. The reason for subtracting rather than omitting these pinch parts is that they contribute with weight 2 to  $\hat{\Delta}_{\mu\nu}$ , because Fig. 1e must be doubled as discussed in connection with (2.10), but with weight 1 to  $\hat{\Gamma}\hat{\Delta}$  via Fig. 3a. Thus we must subtract twice Fig. 3a from the sum of all graphs in order to leave off the pinch parts of  $\hat{\Delta}_{\mu\nu}$ , but the sum of all graphs includes Fig. 3a with unit weight. It is easy to see how this works in connection with (2.22): subtracting the pinch parts adds  $(9/48\pi^2) g^2 \ln(-q^2/\mu^2)$  to this equation, yielding the desired result for  $\hat{\Gamma}$ .

Now to the full calculation. In this section we derive the Ward identity (2.20) by multiplying  $q_1^\mu$  into the sum of the graphs in Figs. 2d, e, f, g, h minus the graphs of Fig. 2c. The vertex itself will be displayed in Section III, and it will be evident from its form that it satisfies (2.20). Fig. 5a shows the vertex graph of Fig. 2d with all momenta and indices labeled, and Fig. 5b expands on Fig. 2g. The notation of Fig. 5, plus the following remarks, enable one to understand the results presented in Table 1, which shows how the various graphs add up to give the Ward identity.

The notation of Table 1 is as follows:

1. The vectors  $k_{\mu i}$  ( $i = 1, 2, 3$ ) are defined in Fig. 5a.
2.  $\Gamma_{\mu\nu\alpha\beta}$ , etc., are the ordinary vertices of Eq. (2.3); their momenta can be read off from Fig. 5a.

3.  $P_{\alpha p}(3) \equiv P_{\alpha p}(q_3)$  (etc.) is the projection operator of (2.17). The indices in parenthesis do not refer to the  $k_{\mu i}$ , but to the  $q_{\mu i}$ .

4. As in (2.15),  $\Pi_{\mu\nu}^0$  is the conventionally-defined proper self-energy in the Feynman gauge.

5. The quantities  $A(i)$ ,  $B(1, 2, 3)$  are defined by:

$$A(i) = \left( \frac{1}{2} N \right) \frac{i q^2}{(2\pi)^4} \int \frac{d^4 k}{k^2 (q_i + k)^2} \quad (2.24)$$

$$B(1, 2, 3) = \left( \frac{1}{2} N \right) \frac{i q^2}{(2\pi)^4} \int \frac{d^4 k}{k_1^2 k_2^2 k_3^2} \quad (2.25)$$

6. The column labeled "3-gluon parts" in Table 1 simply means that the corresponding contribution to  $q_1^\mu \Gamma_{\mu\nu\alpha}$  involves  $B(1, 2, 3)$  with three internal gluon propagators, with an analogous interpretation of "2-gluon parts."

7. The propagators for the  $q_i$  are omitted, as in an overall group-theoretic factor of  $i\epsilon_{abc}$ .

The concise presentation of results in Table 1 conceals a great deal of labor which goes into each entry, including various rearrangements, shifting of integration variables, etc. As we will see in Section III, the computation of even unpinched graphs like Figs. 2d, e, f is materially assisted by using the special vertex decomposition of Eqs. (2.4, 5) into a Feynman part of a pinch part. In particular, this decomposition allows one to see explicitly the cancellation between the ghost graphs (Fig. 2e) and the first line of the entry in Table 1 for Fig. 2d, the ordinary vertex graph. This part of the ordinary vertex graph comes from the pinch-part vertex  $\Gamma^P$  of (2.5). Of course, the  $\Gamma^P$  in Figs. 2g, h are what gives rise to their corresponding pinch parts Fig. 3b. We should note, by the way, that the pinch parts of Figs. 2g, h are equal and opposite except for the overall group-theory factor; thus

this factor becomes a commutator giving rise to a factor of  $i(N/2) \epsilon_{abc}$ . From Table 1 one sees that these pinch parts are essential for the Ward identity; they did not appear in our simplified analysis given earlier because  $A(2)-A(3)$  in Table 1 is independent of the renormalization point  $\mu$ , and the three-gluon parts are convergent also.

Although we have only presented here some of the details of how the Ward identity is satisfied using the S-matrix pinch technique, we have also constructed the full vertex (not just its divergence) with this technique. Since the same answer is found with the intrinsic pinch technique of Section 3, we postpone recording the result for  $\hat{\Gamma}_{\mu\nu\alpha}$  to that section.

### 3. The Intrinsic Pinch Technique.

In this Section we complete the work of Section 2 by giving an explicit expression for the gauge-invariant proper vertex  $\hat{\Gamma}_{\mu\nu\alpha}$  as well as for  $\hat{\Pi}_{\mu\nu}^0$  using a technique which avoids imbedding as much as possible. There is nothing new in principle here; it is just another way of looking at the calculation of the last section. From these expressions it will be entirely elementary to check the Ward identity (2.20).

The general idea is this: Note that the pinch graphs (Figs. 2e,f; 3a,b) are always missing one or more propagators corresponding to the external legs of the improper Green's function in question, e.g.,  $\hat{A}_{\mu\nu}$ . These graphs, as we know, are essential to cancel the gauge dependence of ordinary graphs, e.g., Fig. 2a for  $\hat{A}_{\mu\nu}$ . It follows that the gauge-dependent parts of such ordinary graphs must also be missing one or more external-line propagators. So our goal is to extract systematically the parts of proper graphs which are missing external propagator legs, and simply throw them away. We do this by looking for inverse propagators in proper graphs which arise from Ward identities such as (2.6). (There is one important point to remember: as in the last section, the proper vertex is defined as the sum of Figs. 2d,e,f (the usual graphs), minus the pinch graphs of Fig. 3a.)

#### A. The Proper Self-Energy.

The usual Feynman-gauge proper self-energy of Fig. 6 has the value (for gauge group  $SU(N)$ )

$$\Pi_{\mu\nu}^0(q) = \frac{iNg^2}{2(2\pi)^4} \int \frac{d^4 k}{k^2(k+q)^2} \{ \Gamma_{\alpha\mu\lambda} \Gamma_{\lambda\nu\alpha} - k_\mu(k+q)_\nu - k_\nu(k+q)_\mu \} \quad (3.2)$$

where we symmetrized the ghost loop of Fig. 6b. Now write the vertices as we did in (2.3), in such a way that the external momentum  $q$  is singled out and a

piece of the vertex called  $\Gamma^P$  is constructed that carries only longitudinal (i.e., pinch) terms in the internal momenta:

$$\Gamma_{\alpha\mu\lambda}^F = \Gamma_{\alpha\lambda}^F(k, q, -k-q) = \Gamma_{\alpha\lambda}^F + \Gamma_{\alpha\lambda}^P, \quad (3.3)$$

$$\Gamma_{\alpha\mu\lambda}^F = (2k+q)\Gamma_{\mu\alpha\lambda}^0 - 2q_\alpha q_{\mu\lambda} + 2q_\lambda q_{\mu\alpha}; \quad (3.4)$$

$$\Gamma_{\alpha\mu\lambda}^P = -k_\alpha q_{\mu\lambda} - (q+k)\Gamma_{\mu\alpha}^0.$$

We used this decomposition earlier in the discussion of the vertex graph Fig. 1b from which we extracted the pinch part of Fig. 1e. Now, however, we use it for the normal graph of Fig. 1a. The full vertex  $\Gamma_{\mu\alpha\lambda}$  obeys a Ward identity like (2.20):

$$k_\alpha \Gamma_{\mu\nu\lambda}^0 = d^{-1}(q)\Gamma_{\mu\nu}^0(q) - d^{-1}(q+k)\Gamma_{\mu\nu}^0(q+k) \quad (3.6)$$

with  $d^{-1}(q) = q^2$ , etc. The rules of the intrinsic pinch technique are to let the pinch vertex  $\Gamma^P$  act on the full vertex, and to throw out the  $d^{-1}(q)$  terms thereby generated with the Ward identity (3.6). To this end, write

$$\Gamma_{\mu\alpha\lambda}^F \Gamma_{\nu\alpha\lambda}^0 = \Gamma_{\mu\alpha\lambda}^F \Gamma_{\nu\alpha\lambda}^F + \Gamma_{\mu\alpha\lambda}^P \Gamma_{\nu\alpha\lambda}^0 + \Gamma_{\nu\alpha\lambda}^P \Gamma_{\mu\alpha\lambda}^0 - \Gamma_{\mu\alpha\lambda}^P \Gamma_{\nu\alpha\lambda}^P. \quad (3.7)$$

Of the four terms on the RHS of (3.7), the first is saved in its entirety, as it generates no pinches; the second two contain  $d^{-1}(q)$  terms which we will drop; the fourth plays a role in cancelling the ghost loop. We find, using (3.6):

$$\Gamma_{\mu\alpha\lambda}^F \Gamma_{\nu\alpha\lambda}^0 = 4d^{-1}(q)\Gamma_{\mu\nu}^0(q) - 2\Gamma_{\mu\nu}^0(q+k)d^{-1}(q+k).$$

$$(3.8)$$

The first term on the RHS will be dropped. Note that it has precisely the weight 4 which we found for the pinch graph of Fig. 1e (see Eq. (2.10)), and dropping this term in (3.8) has the same effect as cancelling it with the S-matrix pinch technique.

After some algebra, and using the dimensional-regularization rule (3.1) to drop terms like  $q_{\mu\nu}^2 k^2$  arising from (3.8), the final result is (including the ghost loop, which gets cancelled)

$$\hat{\Gamma}_{\mu\nu}^0(q) = \frac{iq^2 N}{2(2\pi)^4} \int \frac{d^4 k}{k^2 (k+q)^2} \{ \Gamma_{\mu\alpha\lambda}^F \Gamma_{\nu\alpha\lambda}^F - 2(2k+q)\Gamma_{\mu\alpha\lambda}^0 \Gamma_{\nu\alpha\lambda}^0 \}. \quad (3.9)$$

This is the same  $\hat{\Gamma}_{\mu\nu}^0$  as given in Section 2, and it is automatically conserved (because it differs from  $\hat{\Gamma}_{\mu\nu}^0$  by the conserved terms dropped in (3.8)). To see that it is the same, just use the results

$$\Gamma_{\mu\alpha\lambda}^F \Gamma_{\nu\alpha\lambda}^F = -8q^2 \Gamma_{\mu\nu}^0(q) + 4(2k+q)\Gamma_{\mu\alpha\lambda}^0 \Gamma_{\nu\alpha\lambda}^0; \quad (3.10)$$

$$\int \frac{d^4 k}{k^2 (q+k)^2} (2k+q)\Gamma_{\mu\alpha\lambda}^0 \Gamma_{\nu\alpha\lambda}^0 = \frac{1}{3} q^2 \Gamma_{\mu\nu}^0(q) \int \frac{d^4 k}{k^2 (q+k)^2}. \quad (3.11)$$

### B. The 3-Gluon Vertex.

Exactly the same principles apply as for the propagator: Rewrite the three-gluon vertices appearing in the proper vertex graphs in  $\Gamma^F + \Gamma^P$  form (always singling out the external momenta  $q_1$  of Fig. 5a and Fig. 2f for special treatment). Apply the  $\Gamma^P$  to the full vertices, generating terms

involving  $d^{-1}(q_i)$ ; drop these. Note the cancellation between the ghost graphs and the pure  $\Gamma^P$  contributions. Finally, remember to subtract the graphs of Fig. 3a to complete the definition of the proper vertex  $\Gamma_{\mu\nu\alpha}$ .

The contribution of Fig. 5a to the proper vertex  $\Gamma$  is

$$\Gamma_{\mu\nu\alpha}^{(5a)} = \frac{i q^2 N}{2 (q\pi)^4} \int \frac{d^4 k}{k_1^2 k_2^2 k_3^2} N_{\mu\nu\alpha}. \quad (3.12)$$

In recording the numerator  $N_{\mu\nu\alpha}$  we use a compressed notation in which all Lorentz indices are suppressed:

$$N = \Gamma_1^F \Gamma_2^F \Gamma_3^F + \Gamma_1^P \Gamma_2^P \Gamma_3 + \Gamma_1 \Gamma_2^P \Gamma_3 + \Gamma_1^P \Gamma_2^P \Gamma_3 - \Gamma_1^P \Gamma_1^P \Gamma_3 \\ - \Gamma_1^P \Gamma_2^P \Gamma_3 + \Gamma_1^P \Gamma_2^P \Gamma_3. \quad (3.13)$$

Here each vertex labeled 1 carried the indices  $q_{\mu 1}$ , each vertex labeled 2 carries indices  $\lambda \nu \rho$ , and each vertex labeled 3 carries indices  $\rho \sigma \theta$ ; 1, 2, and 3 refer to the external momentum labels. Thus the first term on the RHS of (3.13) really means

$$\Gamma_{q\mu 1}^F(k_2, q_1, -k_3) \Gamma_{\lambda \nu \rho}^F(k_3, q_2, -k_1) \Gamma_{\rho \sigma \theta}^F(k_1, q_3, -k_2) \quad (3.14)$$

using the notation of Eqs. (3.3, 4). As with the propagator, the first term on the RHS of (3.13) contains no pinches, and is saved as is. Each of the next six terms has pinches (i.e., terms in  $d^{-1}(q)$ ) coming from the action of  $\Gamma^P$  on  $\Gamma$ , via the Ward identity (3.6). These  $d^{-1}$  terms can refer to an external momentum  $k_1, 2, 3'$  in which case they give rise to an integral with only two propagators, such as occur in Figs. 2f, 3a. The last term on the RHS of

(3.13), with three  $\Gamma^P$ 's, yields terms of this latter sort as well as a contribution which just cancels the ghost graphs of Fig. 2e;

$$(\Gamma_1^P \Gamma_2^P \Gamma_3^P)_{\mu\nu\alpha} = d^{-1}(k_3) [k_{2\mu} g_{\alpha\nu} + k_{1\nu} g_{\alpha\mu}] \\ + d^{-1}(k_2) [k_{3\mu} g_{\nu\alpha} + k_{1\alpha} g_{\mu\nu}] + d^{-1}(k_1) [k_{3\nu} g_{\mu\alpha} + k_{2\alpha} g_{\mu\nu}] \quad (3.15)$$

Terms with one  $\Gamma^P$  and two  $\Gamma$ 's have no external pinches, e.g.,

$$(\Gamma_1^P \Gamma_2^P \Gamma_3^P)_{\mu\nu\alpha} = k_1^2 [\Gamma_{q\mu 1}^F(k_1, q_3, -k_2) + \Gamma_{\mu\nu\alpha}^F(k_3, q_2, -k_1)] - k_{1\nu} g_{\alpha 1} d^{-1}(k_2) \\ - k_{1\alpha} g_{\mu\nu} d^{-1}(k_3) + k_{1\nu} k_{2\alpha} k_{2\mu} + k_{1\alpha} k_{3\mu} k_{3\nu}. \quad (3.16)$$

So it is only the terms with two  $\Gamma^P$ 's and one  $\Gamma^F$  that have the external pinches that we drop, e.g.,

$$-\Gamma_1^P \Gamma_2^P \Gamma_3 = -\Gamma_{q\mu 1}^F(k_1, q_3, -k_2) d^{-1}(k_3) + k_{3\nu} d^{-1}(k_2) p_{\alpha 1}^{(2)} \\ + k_{3\mu} d^{-1}(k_1) p_{\alpha 1}^{(1)} + \dots \quad (3.17)$$

where the omitted terms have factors of  $d^{-1}(q_1)$  and are to be dropped.

All that remains is to combine the terms from (3.15), 16, 17) that have only two gluon propagators with the other two-gluon parts of Figs. 3a (with a minus sign) and 2f. The final result is

$$\hat{\Gamma}_{\mu\nu\alpha}(q_1, q_2, q_3) = \hat{\Gamma}_{\mu\nu\alpha}$$

$$+ \frac{i g_N^2}{2(2\pi)^4} \int \frac{d^4 k}{k_1^2 k_2^2 k_3^2} ((\Gamma_1^F \Gamma_2^F \Gamma_3^F)_{\mu\nu\alpha} + 2(k_1+k_2)_\mu (k_1+k_3)_\nu (k_2+k_3)_\alpha)$$

$$- \theta(q_{1\alpha} q_{\mu\nu} - q_{1\nu} q_{\mu\alpha}) A(1)$$

$$- \theta(q_{2\mu} q_{\alpha\nu} - q_{2\alpha} q_{\mu\nu}) A(2) - \theta(q_{3\nu} q_{\mu\alpha} - q_{3\mu} q_{\nu\alpha}) A(3) \quad (3.18)$$

where the integrals  $A(i)$  are defined in (2.24). This is the major result of our paper. It is now rather easy to verify the Ward identity (2.20), using the elementary Ward identity (2.6) for the  $\Gamma^F$ ; in this verification, the form (3.9) for  $\hat{\Pi}_{\mu\nu}$  appears in a natural way.

We have calculated the integrals in (3.18) for those terms which require regulation (that is, which depend on the renormalization point  $\mu$ ). They are of the form

$$\hat{\Gamma}_{\mu\nu\alpha} = \Gamma_{\mu\nu\alpha}(1 + bg^2 \ln(-q^2/\mu^2)) + (\text{independent of } \mu) \quad (3.19)$$

where  $q$  is representative of any of the external momenta. Of course, (3.19) is just what we expect; it shows  $\hat{\Gamma}$  having the same renormalization-group properties as  $d^{-1}(q)$ .

#### 4. A Toy Model.

In the previous sections we have computed the invariant vertex  $\hat{\Gamma}$  at one-loop order of perturbation theory. It would be nice to have an analogous one-dressed loop result, which would amount to an SD equation with cubic non-linearity, analogous to the nonlinear one-dressed-loop equation for  $\hat{\Delta}_{\mu\nu}$  of Refs. 1, 2. Although we are working in this direction, unfortunately we have no progress to report. Instead we consider a toy equation, which we essentially pull out of the air, which incorporates some of the crucial features we expect from the as-yet undiscovered real SD equation. These features include asymptotic freedom and the renormalization group correct to one-loop level, but in the context of an equation with cubic non-linearity.

It is the nonlinear features which are of interest, and in spite of the largely ad hoc nature of the model, these turn out to be interesting and realistic.

We ignore all complications of spin, except for the powers of momentum they induce. Thus we think of  $\hat{\Gamma}_{\mu\nu\alpha}$  as having one power of momentum multiplying a dimensionless function which we call  $\hat{\Gamma}$  (cf. (3.19)). In principle  $\hat{\Gamma}$  depends on three momenta, but we approximate it by a function of only one momentum, presumably representative of the case where all three momenta are more or less equal. Finally, the equation for  $\hat{\Gamma}$  will also depend on  $\hat{\Delta}_{\mu\nu}$ , which again we replace by a scalar function  $\hat{d}(q)$  (see (2.19)). In terms of  $\hat{d}$  we define a dimensionless (and positive, in the regime of Euclidean momenta) function  $\hat{z}(q^2)$  by

$$\hat{d}(q^2)^{-1} = q^2 \hat{z}(q^2) \quad (4.1)$$

According to the Ward identity (2.20) we might expect  $\hat{f} = \hat{z}$ , which it turns

out will thwart one obvious simplification of the true SD equation. This is, in Euclidean space,

$$\hat{\Gamma}(q) = z - \frac{bq^2}{\pi^2} \int \frac{d^4 k}{k^2 (q+k)^2} \hat{z}^3(k) \hat{z}^{-3}(k) \quad (4.2)$$

which represents a triangle graph like Fig. 5a but with dressed lines and vertices, and with two powers of momentum in the numerator, coming from spin, cancelling out a propagator factor. But if  $\hat{\Gamma} = \hat{z}$ , Eq. (4.2) simply reduces  $\hat{\Gamma}$  to an uninteresting quadrature, with no possible nonlinear feature. Of course, (4.2) then does give the correct one-loop result

$$\hat{\Gamma}(q) = 1 + b q^2 \ln(q^2/\mu^2) \quad (4.3)$$

but nothing else.

A more promising approach is to use as the subject of the equation a half-proper vertex, defined by (for the moment re-instantiating the full momentum dependence):

$$\hat{G}(q_1, q_2, q_3) = [\hat{z}(q_1) \hat{z}(q_2) \hat{z}(q_3)]^{-1/2} \hat{\Gamma}(q_1, q_2, q_3) \quad (4.4)$$

We might then replace (4.2) by

$$\hat{G}(q) = \hat{z}(z(q))^{-3/2} - \frac{bq^2}{\pi^2} \int \frac{d^4 k}{k^2 (q+k)^2} \hat{z}^3(k) \quad (4.5)$$

where we have paid attention to (4.4) in deciding what factors of  $\hat{z}$  are inside the  $k$ -integral and what factors depend only on external momenta. The ward identity now leads us to expect  $\hat{G} = z^{-1/2}$ , and so (4.5) is indeed an equation

for  $\hat{G}$  with a cubic nonlinearity.

Unfortunately, this equation--while perfectly acceptable at  $O(q^2)$ --leads to problems at higher orders, so we modify it by changing the integral in (4.5) so as to account correctly for the  $\hat{z}^{-3/2}$  term at one-loop order. Our almost-final toy-model equation is:

$$\hat{G}(q) = + \frac{bq^2}{2\pi^2} \int \frac{d^4 k}{k^2 (q+k)^2} \hat{z}^3(k) . \quad (4.6)$$

(The final step will be to remove the infrared singularities coming from the massless propagators, but we defer that step until later.) Changing the coefficient of the integral from  $-bq^2/\pi^2$  to  $+bq^2/(2\pi^2)$  accounts for dropping the first term on the RHS of (4.5), at least at  $O(q^2)$ .

By introducing the variable  $G(q) = g\hat{G}(q)$  it is clear from (4.6) that  $G(q)$  is in fact independent of the coupling constant  $g$ . This is the first step in finding a renormalization-group (RG) equation for  $G$ , which is just the usual running charge.

The simplest way to deal with (4.6) is to find an equivalent differential equation in the variable

$$t = \ln(q^2/\mu^2) \quad (4.7)$$

where  $\mu$  is an arbitrary mass scale. This differential equation is:

$$\dot{\hat{G}} + \dot{G} = - \frac{b}{2} G^3 \quad (4.8)$$

where dots indicate derivatives with respect to  $t$ . One boundary condition is supplied by the normalization  $G(t=0) = g$ , and we also demand that  $G$  vanish as

$t \rightarrow +\infty$ . (Of course, we choose  $\mu$  in such a way that  $G$  is independent of  $g$ , in spite of the normalization condition.) At large  $t$  the  $\hat{G}$  term in (4.8) can be dropped, and we immediately find<sup>22</sup>

$$G = g(1+bg^2 t)^{-1/2}, \quad (4.9)$$

the usual one-loop result for the running charge.

Even though the basic equation (4.6) would appear to be justified only to  $O(g^2)$ , let us work out higher-order terms. Write  $G = gL^{-1/2}$ ; it is elementary to work out the expansion

$$L = 1 + bg^2 t + \frac{3}{2} bg^2 \ln(1+bg^2 t) + \dots. \quad (4.10)$$

Compare this to the solution of the RG equation for the usual running charge, to  $O(G^5)$ :

$$\dot{G} = \frac{1}{2} \beta(g) = -\frac{b_1}{2} G^3 - \frac{b_1}{2} G^5 + \dots \quad (4.11)$$

$$G = g\{1 + bg^2 t + (b_1/b) g^2 \ln(1+bg^2 t) + \dots\}^{-1/2}. \quad (4.12)$$

Our equation (4.6), even though "derived" from one-loop considerations, has a RG and a  $\beta$ -function to all orders in  $g$ . Of course, one cannot expect a one-loop equation to know about an  $O(g^4)$  effect with quantitative precision, but it does fairly well: for (4.6), the coefficient  $b_1$  is clearly  $3b_{12}/2$ , while the exact two-loop result (independent of the gauge group for a pure gauge theory) is  $b_1 = 102b_{12}/121$ . The toy-model  $b_1$  is thus about 80% too large. One might compare this to other non-perturbative approaches to QCD based on the gauge

technique for the propagator,<sup>15</sup> which have RG's for which the  $O(g^3)$  term in  $\beta$  is given to this accuracy. In contrast, the present model automatically gets this term right, and does as well for the  $O(g^5)$  term as the gauge technique does for the  $O(g^3)$  term.

We will now construct the exact  $\beta$ -function for our toy model. By taking the  $t$ -derivative of (4.11) we can eliminate  $\dot{G}$  from the fundamental equation (4.6), and of course (4.11) itself allows  $\dot{G}$  to be replaced by  $(1/2)\beta$ . Thus from these two equations we derive

$$\beta(g) \left( 1 + \frac{1}{2} \frac{d\beta}{dg} \right) = -bg^3 \quad (4.13)$$

subject to  $\beta \rightarrow -bg^3$  as  $g \rightarrow 0$ . This equation is easily solved as a power series in  $g$ ; the first seven terms are

$$\beta = -bg^3 - \sum_1 b_N g^{2N+3};$$

$$b_1 = (3/2)b^2, \quad b_2 = 6b^3, \quad b_3 = \left(\frac{285}{8}\right)b^4, \quad b_4 = \left(\frac{1071}{4}\right)b^5,$$

$$b_5 = \left(\frac{37989}{16}\right)b^6, \quad b_6 = \left(\frac{47835}{2}\right)b^7. \quad (4.14)$$

The leading term in the recursion relation is

$$b_{N+1} = (N+3) bb_N + \dots \quad (4.15)$$

where the omitted terms are positive; this shows that  $b_N$  grows factorially. A numerical fit shows that for large  $N$

$$b_N = .118 \cdot (1.26b)^{N+1} \cdot (N+2)! \quad (4.16)$$

directly from the perturbative solution (4.10).

Unfortunately this series cannot be Borel-summed, because the signs do not alternate. The factorial growth and uniform sign is just what is expected of QCD; it implies that the running charge  $G$ , to which this  $\beta$ -function applies, is singular for some finite values of  $t$ , and that non-perturbative effects (terms like  $\exp(-1/bg^2)$ ) will be important.

We have solved Eq. (4.13) for  $\beta$  numerically, using  $b$  for QCD<sup>23</sup> ( $b = 11(16\pi^2)^{-1}$ ), with results shown in Fig. 7. In spite of the fact that all of the power-series coefficients in  $\beta$  are negative,  $\beta$  turns around and has a zero at  $g \approx 5$  (for  $SU(3)$ ). This is easy to understand: From (4.13)

$$\beta' = 2 \left[ -1 + \frac{\ln^3}{|\beta|} \right] > -2 \quad (4.17)$$

which implies  $0 > \beta > -2g$ . Then (4.17) implies that as long as  $\beta' \leq 0$  it satisfies  $|\beta'| < 2-bg^2$ . Thus  $\beta'$  will vanish somewhere near  $g \lesssim (2/b)^{1/2}$ , and for larger values of  $g$ ,  $\beta'$  is positive. Eq. (4.13) shows that the approach to  $\beta = 0$  is a square-root singularity:  $\beta \sim (g_c - g)^{1/2}$ . For  $g > g_c$ ,  $\beta$  is imaginary and our equations make no sense; we have reached an inescapable singularity of both  $\beta$  and  $G$ .

This problem, and its singular behavior, has a mechanical analog. Eq. (4.8) is the equation of motion for a particle of coordinate  $G$  in a potential  $\sim bG^4$ , with frictional damping. The generic solution has the particle undergoing damped oscillations about  $G = 0$ , finally coming to rest at  $G = 0$  when  $t = \infty$ . However, for QCD we require that  $\beta$  (and also  $\dot{G}$ , from (4.11)) are always negative, so that  $G$  reaches zero only once, at  $t = +\infty$ . This non-generic solution is singular sufficiently far in the past, as can be seen

This singularity comes from having massless propagators. In the integral equation (4.6), if  $G$  is always of one sign then the integral on the RHS is singular at least at  $q = 0$  ( $t = -\infty$ ). In fact, gluons do have a constituent mass,<sup>1,2,17</sup> so the obvious way to remove the singularities of (4.6) is to write instead

$$G(q) = \frac{b}{2\pi^2} \int d^4 k \frac{G^3(k)}{(k^2+m^2)[(k+q)^2+m^2]} \quad (4.18)$$

There is no simple differential equation anymore for  $G$ , such as (4.8); instead, we can integrate out the angular variables in (4.17) and solve the resulting one-dimensional integral equation numerically. To make contact with perturbative QCD for  $q \gg m$ , we still want to identify

$$G(q/\mu) = g(\mu) \quad (4.19)$$

when  $\mu \gg m$ . Clearly  $G$  depends only on  $(q/m)$ , so  $g(\mu)$  should be written as  $g(\mu/m)$ . Usually we write  $g$  as a function of  $\mu/\Lambda_{RG}$ , e.g., at one loop

$$g^2(\mu) = [b \ln(\mu^2/\Lambda_{RG}^2)]^{-1} \quad (4.20)$$

or equivalently

$$g^2(\mu) = [b \ln(\xi^2 \mu^2/m^2)]^{-1} \quad (4.21)$$

$$\xi^2 = m^2/\Lambda_{RG}^2$$

By choice of  $\xi$  we impose a normalization condition on  $G$  at large momentum. Large values of  $\xi$  present no problem; by (4.18) and (4.20) this means that  $G$  is small at large  $q$ . But the RHS of (9.17) still manages to be as big as the LHS because the integral is nearly divergent. Small values of  $\xi$  are a different question, since this yields a large value for  $G(q=\mu)$  and there is no way the LHS of (4.17) can be as big as the RHS. We have solved (4.17) numerically, with results presented in Fig. 8 for  $\xi \geq 2.5$ . For smaller values of  $\xi$  the calculations are very delicate to do, but it is evident that for  $\xi$  less than some critical value  $\xi_c$  there is no solution any more. An excellent fit (a few percent or better) to  $\alpha_s(0)$  as shown in Fig. 8 is

$$\alpha_s(0) = \frac{G^2(q=0)}{4\pi} = [4\pi b \ln(1.7\xi^2)]^{-1} . \quad (4.22)$$

Taken literally, (4.22) suggests that  $\xi_c \approx 0.78$ . However, this formula is not accurate for  $\xi < 2$ , and the best one can say is that  $\xi_c$  is  $1.5 \pm .5$ , more or less. Earlier work<sup>1,2</sup> using the gauge technique for the new propagator, gave specific estimates for the gluon mass (which we cannot do with (4.18)), other than to say  $\xi > \xi_c$  which amounted to  $\xi \approx 2 \pm 0.5$ . Note from Fig. 8 that  $\xi = 2.5$  corresponds to  $\alpha_s(0) \approx 0.5$ , representative of fits to the  $\alpha_s/r$  part of quarkonium potentials. For this value of  $\xi$  the running charge as plotted in Fig. 8 is reasonably consistent with the earlier work<sup>1,2</sup> which established the running charge from the propagator rather than from the vertex. Thus there is rough consistency between these different approximation schemes.

The solution to (4.17) gives the running charge for all momenta from 0 to  $\infty$ . We can use this solution to define a  $\beta$ -function via (as in (4.11))

$$\beta(g) = q \frac{d}{dq} G(q) \quad (4.23)$$

where on the RHS  $q$  is eliminated in favor of  $G$  after differentiating. This  $\beta$ -function will resemble that of Fig. 7 at small  $g$ , but at larger  $g$  it is a new and non-perturbative constant, having nothing to do with the renormalization group. Given  $G(q)$  this  $\beta$ -function is superfluous, but is of heuristic interest for comparison with other constructs. We plot  $\beta(g)$  as derived from (4.23) in Fig. 9 for various values of  $\xi$ . Note that the rough shape is the same as the massless  $\beta(g)$  from Fig. 7, but the actual values are much smaller; moreover, the infrared fixed points of Fig. 9 have finite slopes. These fixed points occur at  $q = 0$ , where  $\beta$  for (4.23) automatically vanishes since  $dG/dq$  is finite at  $q = 0$ .

#### Acknowledgments.

This work was supported in part by the National Science Foundation under Grant PHY-86-13210. One of us (J.P.) thanks S. Chaudhury for assistance with the numerical computations.

## References.

1. J. M. Cornwall, French-American Seminar on Theoretical Aspects of QCD (Marseille, June 1981).
2. J. M. Cornwall, Phys. Rev. D26, 1453 (1982).
3. J. M. Cornwall, W.-S. Hou, and J. E. King, Phys. Lett. 153B, 173 (1988).
4. S. Nadkarni, Phys. Rev. Lett. 61, 396 (1988).
5. Introduced long ago by A. Salam, Phys. Rev. 130, 1287 (1963); R. Delbourgo and A. Salam, *ibid.* 135, B1398 (1964). For modern treatments in the context of QCD, see Refs. 6, 7.
6. J. M. Cornwall and W.-S. Hou, Phys. Rev. D34, 585 (1986).
7. M. Baker, J. S. Ball, and F. Zachariasen, Nucl. Phys. B186, 531; 560 (1981).
8. J. E. King, Phys. Rev. D27, 1621 (1983).
9. B. Haeri, Phys. Rev. D38, 3799 (1988).
10. The conventional one-loop vertex has been given for general momenta in the Feynman gauge by J. S. Ball and T.-W. Chiu, Phys. Rev. D22, 2550 (1980), and for special momenta in a general gauge by W. Celmaster and R. J. Gonsalves, *ibid.* 20, 1420 (1979).
11. J. M. Cornwall, Physica
12. G. 't Hooft, Nucl. Phys. B33, 173 (1971).
13. J. M. Cornwall and G. Tiktopoulos, Phys. Rev. D15, 2937 (1977).
14. Such a homogeneous SD equation suggests that non-Abelian gauge bosons can be thought of as composite, a viewpoint supported by the demonstration that such bosons automatically lie on Regge trajectories in perturbation theory. See, e.g., J. M. Cornwall and G. Tiktopoulos, in *New Pathways in High-Energy Physics II*, ed. A. Perlmutter (Plenum, NY, 1977), p. 213; M. T. Grisaru and H. J. Schnitzer, Phys. Rev. D20, 784 (1979).
15. In the gauge technique (see Refs. 6, 7 and works cited therein) there is also a renormalization group, but even the  $\text{O}(\beta^3)$  term in  $\beta$  comes out wrong, by a factor of up to two. This is because the gauge technique as used in these works ignores the transverse vertex, which is important for the ultraviolet behavior.
16. G. 't Hooft, in *Deeper Pathways in High-Energy Physics*, ed. A. Perlmutter and C. F. Scott (Plenum, NY, 1977), p. 699.
17. C. Bernard, Phys. Lett. 108B, 431 (1982); J. Mandula and M. Ogilvie, *ibid.* B105, 127 (1987); R. Gupta et al., Phys. Rev. D36, 2813 (1987).
18. J. M. Cornwall, Nucl. Phys. B157, 392 (1979).
19. We are not interested in mass dependence coming from internal test-particle loops, which are in any case gauge-invariant and will be omitted.
20. The quantity  $A$  will be constructed uniquely from the Feynman rules given later. From the S-matrix point of view, uniqueness of  $A$  (or equivalently, of  $B$  and  $T_R$ ) can be established by appealing to the analytic properties of  $T$  jointly in the external masses and in  $s, t$ , incorporating all  $t$ -dependent subtraction terms in  $A$ .
21. We do not assume that the pinch graphs of Fig. 3 couple to the quarks via  $\gamma_\mu'$  as given in (2.21); by explicit calculations,  $\gamma_\mu'$ -coupling is what emerges. A little familiarity with the pinch technique will convince the reader that this must be so in general.
22. That (4.9) solves (4.6) in lowest order can be verified by doing the integrals in (4.6) with the techniques given in the Appendix of J. M. Cornwall and R. Shellard, Phys. Rev. D18, 1216 (1978).

23. To use these results for other groups, note that  $\beta/g$  is a universal function of the variable  $bg^2$ .

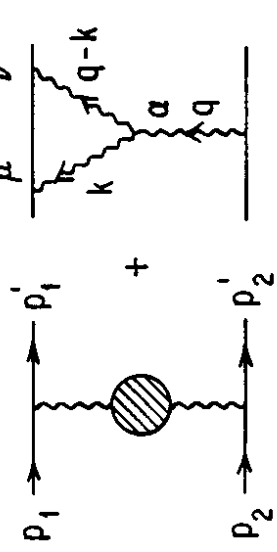
**Table Caption.**

Table 1. Numerators contributing to the Ward identity  $q_1^\mu \Gamma_{\mu\nu\alpha}$ .

**Figure Captions.**

- Fig. 1. Graphs a,b,c are some of the contributions to the S-matrix  $T$ . Graphs e,f are pinch parts which when added to the ordinary propagator parts (d) give a gauge-invariant effective propagator.
- Fig. 2. Some improper vertex graphs in the three-body S-matrix. Graph e is a ghost-loop graph.
- Fig. 3. Pinch parts of the graphs in Fig. 2.
- Fig. 4. Graphical structure of the gauge-invariant S-matrix part  $\tilde{T}$  which is independent of external-particle masses.
- Fig. 5. Some graphs of Fig. 2 indicating momenta and Lorentz indices.
- Fig. 6. Graphs for the ordinary proper self-energy  $\Pi_{\mu\nu}^0$ ; b is a ghost graph.
- Fig. 7. Massless  $\beta$ -function as defined by the solution to (4.13). Also plotted is the perturbative  $\beta$ -function  $-bg^3$  which passes through the minimum of  $\beta$ .
- Fig. 8. Running coupling  $\alpha_s(q) = G^2(q)/4\pi$  for various values of  $\xi = m/\Lambda_{RG}$ . Also plotted is the perturbative value  $(4\pi b \ln(q^2/\Lambda_{RG}^2))^{-1}$ .
- Fig. 9.  $\beta$ -function derived from the solution to (4.16), for various values of  $\xi$ . Also plotted is the perturbative value  $-bg^3$ .

$$T(s, t, M_1, M_2) =$$



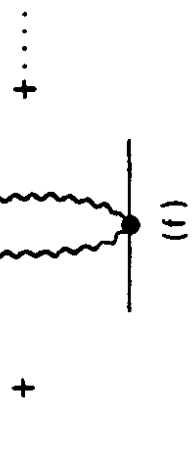
(b)

(c)

$$\hat{f}(t) =$$

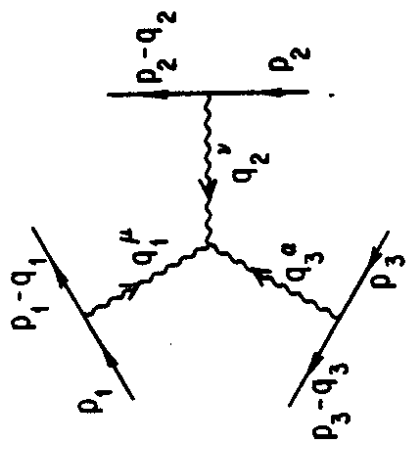
(d)

(e)

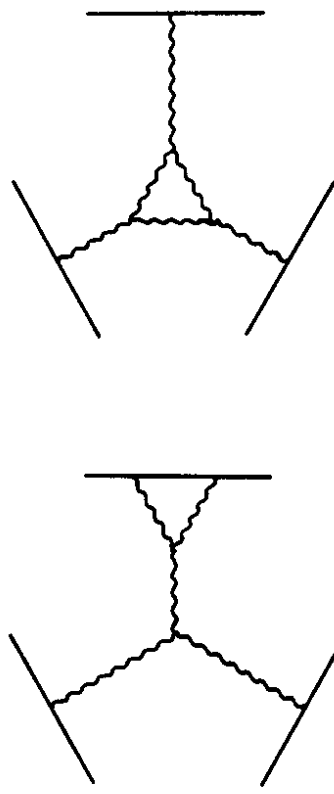


Cornwall and Papavassiliou  
Fig. 1

$$+ \dots$$



(b)  
(three graphs)



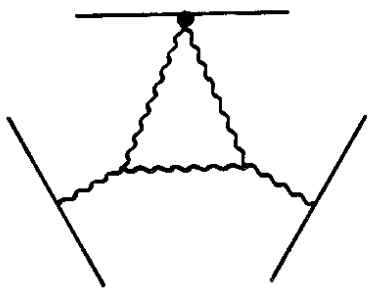
(c)  
(three graphs)

(d)

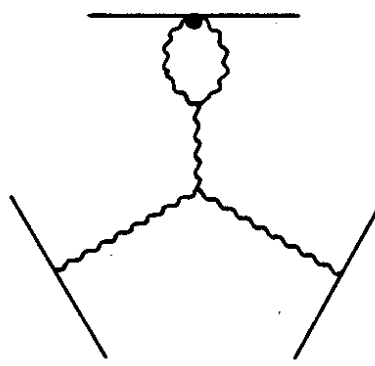
Cornwall and Papavassiliou  
Fig. 2

Cornwall and Papavassiliou  
Fig. 3

(b)  
(three graphs)

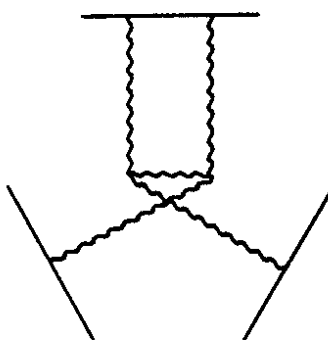


(a)  
(three graphs)

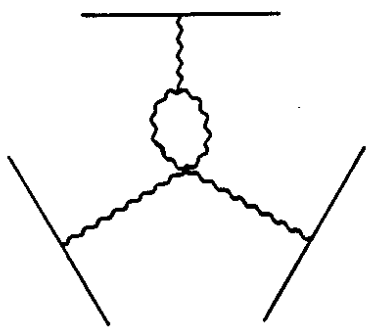


Cornwall and Papavassiliou  
Fig. 2 (cont'd)

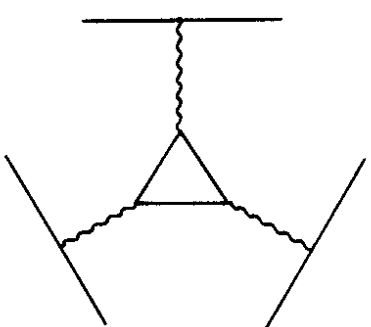
(h)  
(three graphs)



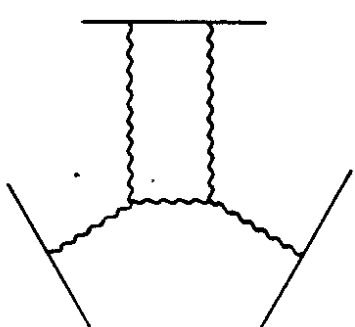
(f)  
(three graphs)

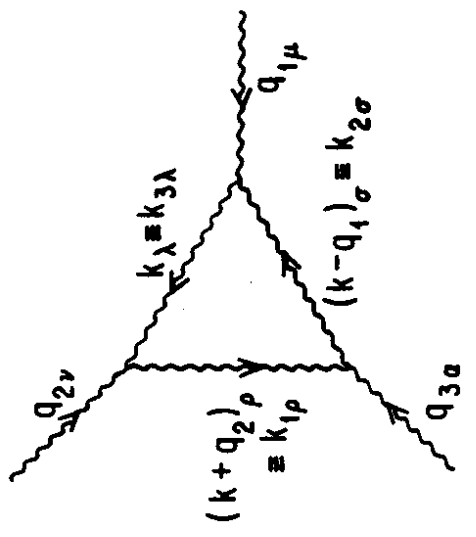


(e)  
(two graphs)

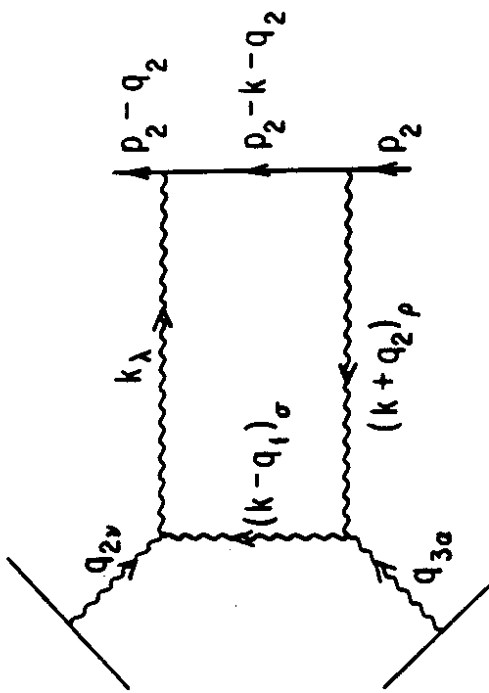


(g)  
(three graphs)



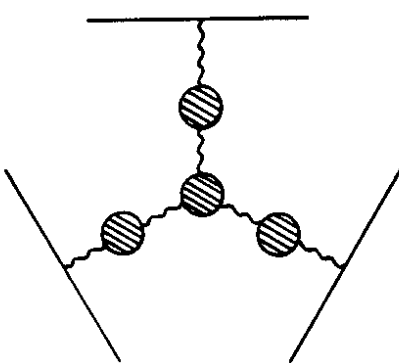


(a)



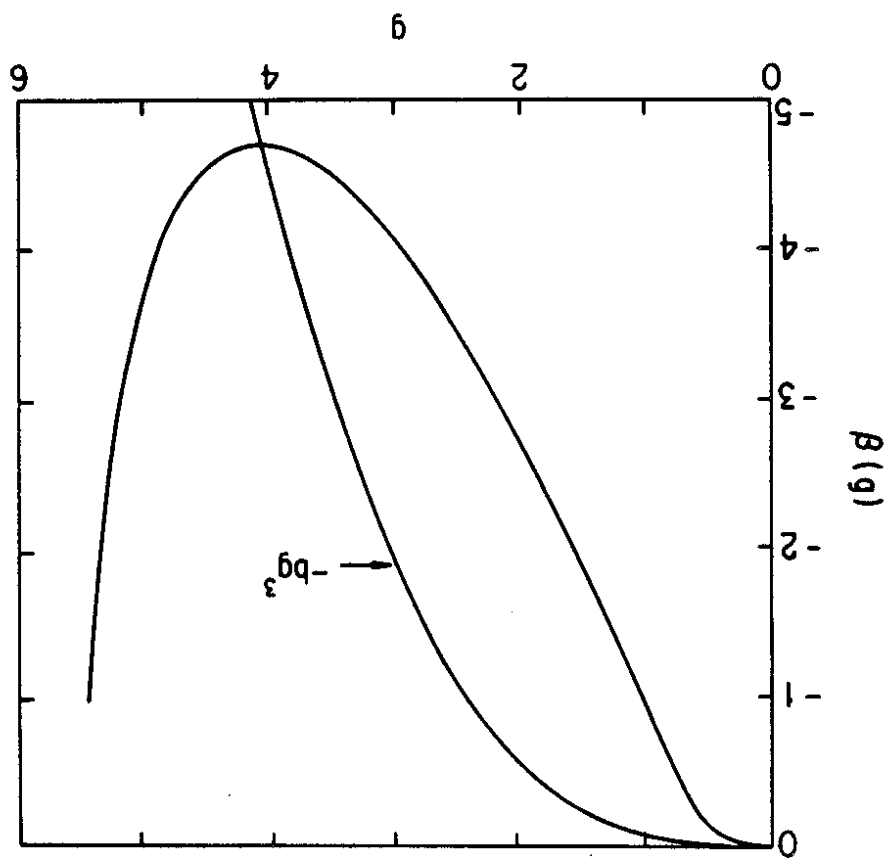
(b)

Cornwall and Papavassiliou  
Fig. 5

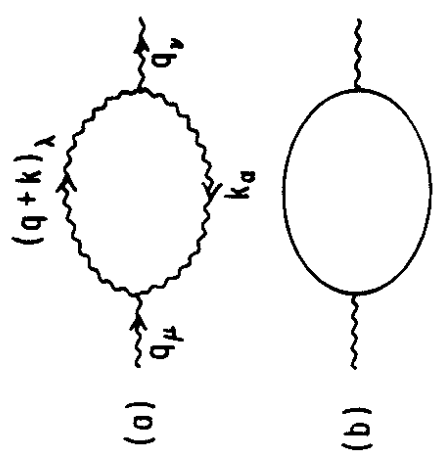


Cornwall and Papavassiliou  
Fig. 4

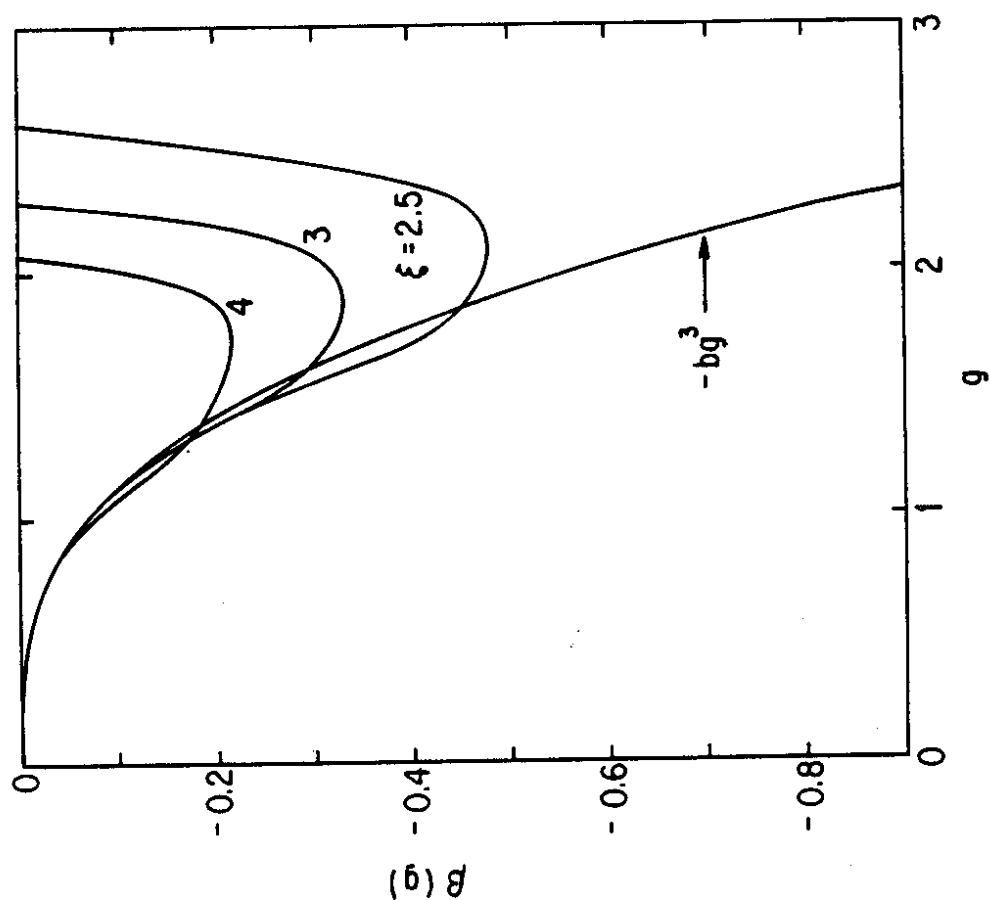
Cornwall and Papavassiliou  
Fig. 7



Cornwall and Papavassiliou  
Fig. 6



Cornwall and Papavassiliou  
Fig. 9



Cornwall and Papavassiliou  
Fig. 8

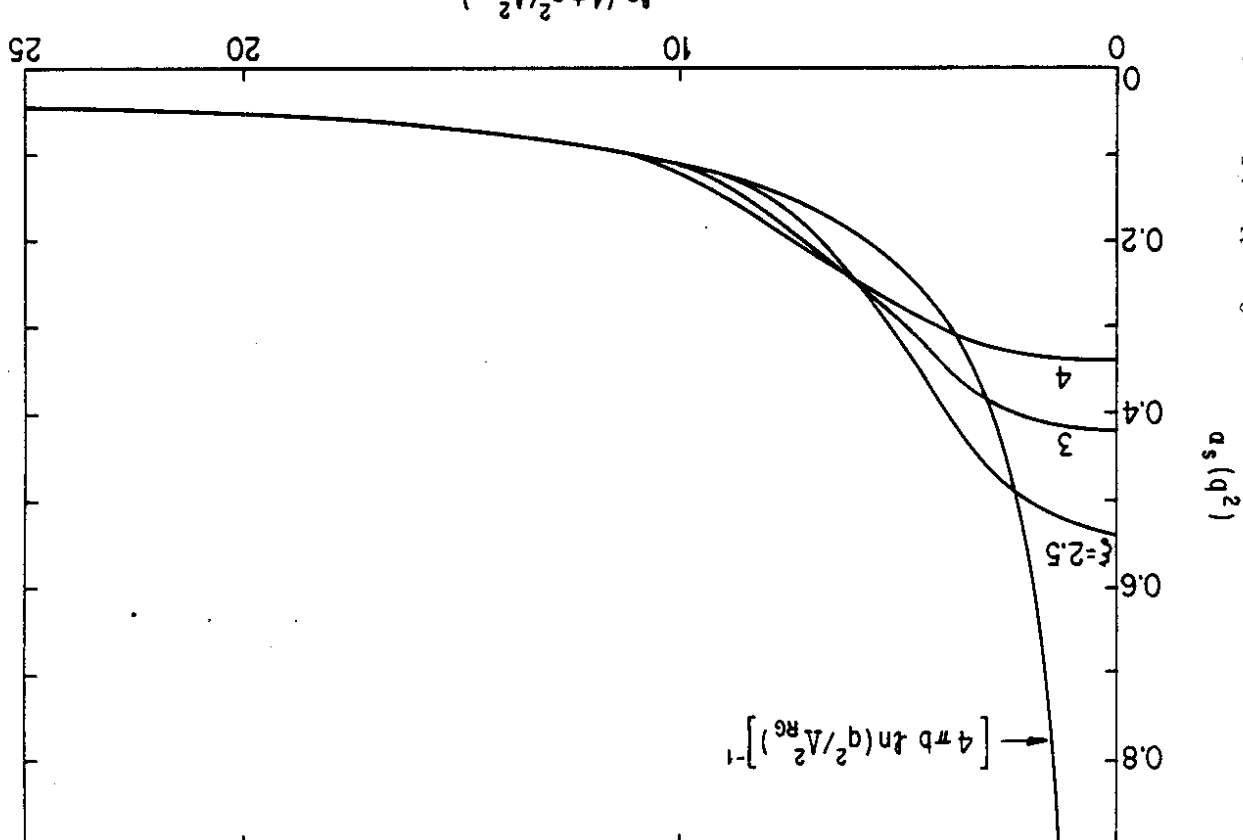


Table 1

<u>Graph</u>	<u>3-Gluon Parts (to be multiplied by <math>B(1,2,3)</math>)</u>	<u>2-Gluon Parts</u>
Fig. 2d	$-q_{1\mu} [k_{3\mu} k_{1v} k_{2\alpha} + k_{2\mu} k_{3v} k_{1\alpha}]$ $-P_{vp}(2) [q_{1\sigma} \Gamma_{\rho\alpha\sigma} + q_{3\rho} k_{1\alpha}]$ $-P_{\alpha\rho}(3) [q_{1\lambda} \Gamma_{\lambda\nu\rho} + q_{2\rho} k_{1v}]$	$2\Pi_{v\alpha}^o(2) - 2\Pi_{v\alpha}^o(3)$ $-2A(1) [P_{v\alpha}(2) - P_{v\alpha}(3)]$
Fig. 2e (2 graphs)	$q_{1\mu} [k_{3\mu} k_{1v} k_{2\alpha} + k_{2\mu} k_{3v} k_{1\alpha}]$	
Figs. 2g,h (2x3 graphs) (pinch part only)	$P_{vp}(2) [q_{1\sigma} \Gamma_{\rho\alpha\sigma} + q_{3\rho} k_{1\alpha}]$ $+P_{vp}(3) [q_{1\lambda} \Gamma_{\lambda\nu\rho} + q_{2\rho} k_{1v}]$	$2[P_{v\alpha}(2) + P_{v\alpha}(3)] [A(2) - A(3)]$
Fig. 2f (2 graphs)	O	$-\Pi_{v\alpha}^o(2) + \Pi_{v\alpha}^o(3)$
Fig. 2c (3 graphs) (pinch parts only x-1)	O	$2[P_{v\alpha}(2) - P_{v\alpha}(3)] [A(1) + A(2) + A(3)]$
SUM	O	$P_{v\alpha}(2) \hat{\Pi}(2) - P_{v\alpha}(3) \hat{\Pi}(3)$